AEE 3162 Summer 2026 Term Project

ML 2D Rocket Engine Nozzle

By Scott Meeson

Table of Contents

1. Introduction

A minimum-length, 2-dimensional rocket engine nozzle was designed to discharge air from a stagnation temperature (T_0) of 1000 K and a stagnation pressure (P_0) of 1500 kPa into an ambient-pressure (P_a) atmosphere of 101 kPa. A nozzle contour was generated using the Method of Characteristics (MOC), producing a diverging section that yields a uniform, parallel, shock-free flow at the exit plane. All calculations and the nozzle design procedure were implemented in a MATLAB program developed for this project (code attached). The prescribed flow conditions and selected design parameters (r_t, n) are summarized in Table 1.

Table 1: Flow Conditions and Design Parameters

Variable	**Description**	**Value**
T_0	Stagnation Temperature	1000 K
P_0	Stagnation Pressure	1500 kPa
$P_a = P_e$	Ambient Pressure	101 kPa
γ	Specific Heat Ratio (Air)	1.4
R	Ideal Gas Constant (Air)	287 J/kgK
r_t	Nozzle Throat Radius	0.02 m
n	Number of Characteristics	50

2. Exit Speed and Exit Mach Number

To calculate M_e, we can use the isentropic relation for P_0/P, where P is the ambient pressure:

$$\frac{P_0}{P} = (1 + \frac{\gamma-1}{2}M_e^2)^{\frac{\gamma}{\gamma-1}}$$

Plugging in,

$$\frac{1500}{101} = (1 + \frac{0.4}{2}M_e^2)^{\frac{1.4}{0.4}}$$

$$\Rightarrow M_e = 2.4101$$

Exit temperature is found with:

$$T_e = \frac{T_0}{1+\frac{\gamma-1}{2}M_e^2} = \frac{1000}{1+0.2(2.41)^2} = 462.6032\ K$$

The local exit speed of sound is then:

$$a_e = \sqrt{\gamma R T_e} = \sqrt{(1.4)(287)(462.6032)} = 431.131\ m/s$$

Then the exit velocity, V_e, is:

$$V_e = M_e a_e = (2.4101)(431.131) = 1,039.053\ m/s$$

3. Kinetic Energy to Specific Stagnation Enthalpy Percentage

The specific heat capacity at constant pressure is:

$$C_p = \frac{\gamma R}{\gamma-1} = \frac{(1.4)(287)}{0.4} = 1004.5\ J/kg \cdot K$$

The specific stagnation enthalpy, h_0, is then:

$$h_0 = C_p T_0 = (1004.5)(1000) = 1,004,500\ J/kg$$

The specific kinetic energy at the exit plane is:

$$KE_{spec} = \frac{1}{2}V_e^2 = \frac{1}{2}(1,039.053)^2 = 539,815.1\ J/kg$$

The percentage of enthalpy converted is then:

$$\% = \frac{KE_{spec}}{h_0} \times 100\% = \frac{539,815,1}{1,004,500} \times 100\% = 53.74\%$$

This 53.74% represents the thermodynamic limit of kinetic energy recovery for this specific pressure ratio ($\frac{P_0}{P_e} = 14.85$). To achieve a higher percentage, the ambient pressure would need to be lower. To do so, expanding into a vacuum where $P_e \rightarrow 0$ and the kinetic-energy fraction approaches 100% would work. Expanding below 101 kPa at sea level would cause the nozzle to be overexpanded, leading to flow separation and a severe loss of efficiency.

4. Method Of Characteristics

4.1 Design

The nozzle shape is designed based on the assumptions that the flow is steady, two-dimensional, irrotational, and isentropic (without shocks). Under such assumptions, the characteristics for the flow field can be found from two groups of lines along which the governing PDEs simplify to algebraic equations. In a left-running characteristic (C^+, upward-sloping line), the quantity:

$$K_+ = \theta - \nu(M)$$

is invariant, while along a right-running characteristic (C^-, sloping down and to the right)

$$K_- = \theta + \nu(M)$$

is invariant. Here θ is the local flow angle measured from the nozzle centerline, and $\nu(M)$ is the Prandtl-Meyer function

$$\nu(M) = \sqrt{\frac{\gamma+1}{\gamma-1}} arctan(\sqrt{\frac{\gamma-1}{\gamma+1}(M^2 - 1)} - arctan(\sqrt{M^2 - 1})$$

which gives the total isentropic turning angle needed to accelerate the flow from sonic conditions to Mach number M. Wherever a C^+ and a C^- line cross, the two invariants can be solved simultaneously:

$$\theta = \frac{K_- + K_+}{2}, \ \nu = \frac{K_- - K_+}{2}$$

After which, the local Mach number is numerically inverted $\nu(M)$, and the Mach angle $\mu = sin^{-1}(1/M)$ locates the characteristic direction. Physically, each characteristic segment is a Mach wave, so between two adjacent grid points, its direction is taken as $tan(\theta - \mu)$ for a C^- line and $tan(\theta + \mu)$ for a C^+ line. Because θ and μ both vary continuously along the true (curved) characteristic, each straight-line segment in the numerical mesh uses the average of $\theta \mp \mu$ evaluated at its two endpoints, which keeps the scheme second-order accurate as the mesh is refined.

Rather than gradually turning the flow along a curved wall, the shortest possible nozzle concentrates the entire expansion into a single, centered fan at the throat lip. Because the centerline cannot support any flow angle other than $\theta = 0$, only half of the total available turning, $\nu_{max} = \nu(M_e)$, can be assigned to the wall. The rest is used up, turning the flow back to zero by the exit. This fixes the maximum wall angle:

$$\theta_{max} = \frac{\nu(M_e)}{2} = \frac{36.99}{2} = 18.495°$$

To approximate the continuous fan numerically, it is discretized into n=50 distinct right-running (C^-) waves, each departing the corner with a prescribed angle $\theta_i = id\theta$, $d\theta = \theta_{max}/n = 0.3699°$. Since the throat is exactly sonic ($\theta = \nu = 0$), the simple-wave relation collapses to $\nu_i = \theta_i$ for every wave, so its governing invariant is simply $K_{-,i} = 2\theta_i$.

There are three point types in the remaining grid. Axis points satisfy the symmetry condition $\theta = 0$, hence their Prandtl-Meyer angle is defined by whichever C^- wave touches the axis, $\nu = K_-$. The reflected wave from that point would carry $K_+ = -\nu$. Interior points are normal intersections of a single C^- and a single C^+ wave, using the equations for θ and ν. Wall points are an exception because, having reached the last C^- wave originating at the corner, there are no more C^- waves left to be intersected. The state entering the wall point is the same as the state of the last interior point on the same characteristic. In other words, the wave is absorbed, not reflected. Ensuring that the wall at every point is locally tangent to the flow direction (considering the wall slopes as the arithmetic average of the incoming and outgoing ones) exactly means canceling all waves at the boundaries, which is the fundamental condition keeping this nozzle free of any shocks and as short as possible. However, the separation between the corner and line is small enough that the flow condition is assumed to be unreflected for the single characteristic closest to the centerline, using the same convention used by Anderson in his worked example problem. This is anticipated to be a relatively minor component of the total discretization error, as discussed in Section 5.1.

This iterative procedure yields a total of $\frac{n(n+3)}{2} = 1325$ grid points, as well as n+1 points defining the physical wall, where the wall inclination decreases in 50 steps of just $0.3699°$ each, starting from an initial value of $\theta_{max} = 18.495°$ until reaching 0°. This produces a wall profile that is smooth and steadily curved at all points downstream of the throat lip. The inevitable exception is the sharp corner formed at the throat itself, which is inherent in a minimum-length configuration.

4.2 Sample Calculation

For point 1,

$$\theta_1 = d\theta = 0.3699° \qquad\qquad K_-^1 = 2\theta_1 = 0.7398° \text{ (along } C_-\text{)}$$

Along the throat,

$$K_+ = \theta - \nu = 0$$

To determine the Mach number, the inverse Prandtl-Meyer relation was solved using a Newton-Raphson iteration until successive estimates differed by less than 10^{-12}.

$$\nu(M) = 0.3699° \Rightarrow M_1 = 1.0414$$

$$\mu_1 = arcsin(\frac{1}{M_1}) = arcsin(\frac{1}{1.0414}) = 73.7807$$

Then, utilizing the single-unkown method,

$$x_1 = 0 - \frac{r_t}{tan(\theta_1 - \mu_1)} = 0.00596\, m\, ,\ y_1 = 0\, m$$

For points 2 and 3, K_+ is still 0, since C^+ is still in the same "row" as point 1. However, we are crossing a new C^- line, so points 2 and 3 each carry their own $K_- = 2\theta_j$.

For point 2,

$$\theta_2 = 2d\theta = 0.7398° \qquad K_-^2 = 2\theta_2 = 1.4796°$$

As K_+ is still 0,

$$\theta_2 = \nu_2 = 0.7398°$$

$$\nu(M) = 0.7398° \Rightarrow M_2 = 1.0665$$

$$\mu_2 = arcsin(\frac{1}{M_2}) = arcsin(\frac{1}{1.0665}) = 69.6607°$$

For point 3,

$$\theta_3 = 3d\theta = 1.1097° \qquad K_-^3 = 2\theta_3 = 2.2194°$$

As K_+ is still 0,

$$\theta_3 = \nu_3 = 1.1097°$$

$$\nu(M) = 1.1097° \Rightarrow M_3 = 1.0879$$

$$\mu_3 = arcsin(\frac{1}{M_3}) = arcsin(\frac{1}{1.0879}) = 66.8081°$$

For points 2 and 3, both the x and y coordinates were computed in code.

Table 2: Sample Calculation Summary

Point	K_- **(°)**	K_+ **(°)**	**θ (°)**	**ν (°)**	**M**	**μ (°)**	**x (m)**	**y (m)**
1	0.7398	0.0000	0.3699	0.3699	1.0414	73.7807	0.00596	0.00000
2	1.4796	0.0000	0.7398	0.7398	1.0665	69.6607	0.00675	0.00248
3	2.2194	0.0000	1.1097	1.1097	1.0879	66.8081	0.00728	0.00387

5. Results

5.1 Nozzle Contour

The resulting design has a nozzle length of $L = 0.158848\ m$ ($L/r_t = 7.94$) and an exit half-height of $y_e = 0.048360\ m$. Dividing by the throat radius gives an area ratio of $A_e/A_t = y_e/r_t = 2.418$, compared with the one-dimensional isentropic value of 2.4254 for $M_e = 2.4101$, a difference of only 0.305%. This discrepancy can be attributed to the 50-wave discretization of the expansion fan, not to any mistakes in the theory. It should become smaller as more characteristics are used to describe the expansion fan. The contour of the wall with the grid of characteristic lines is depicted in Figure 1.

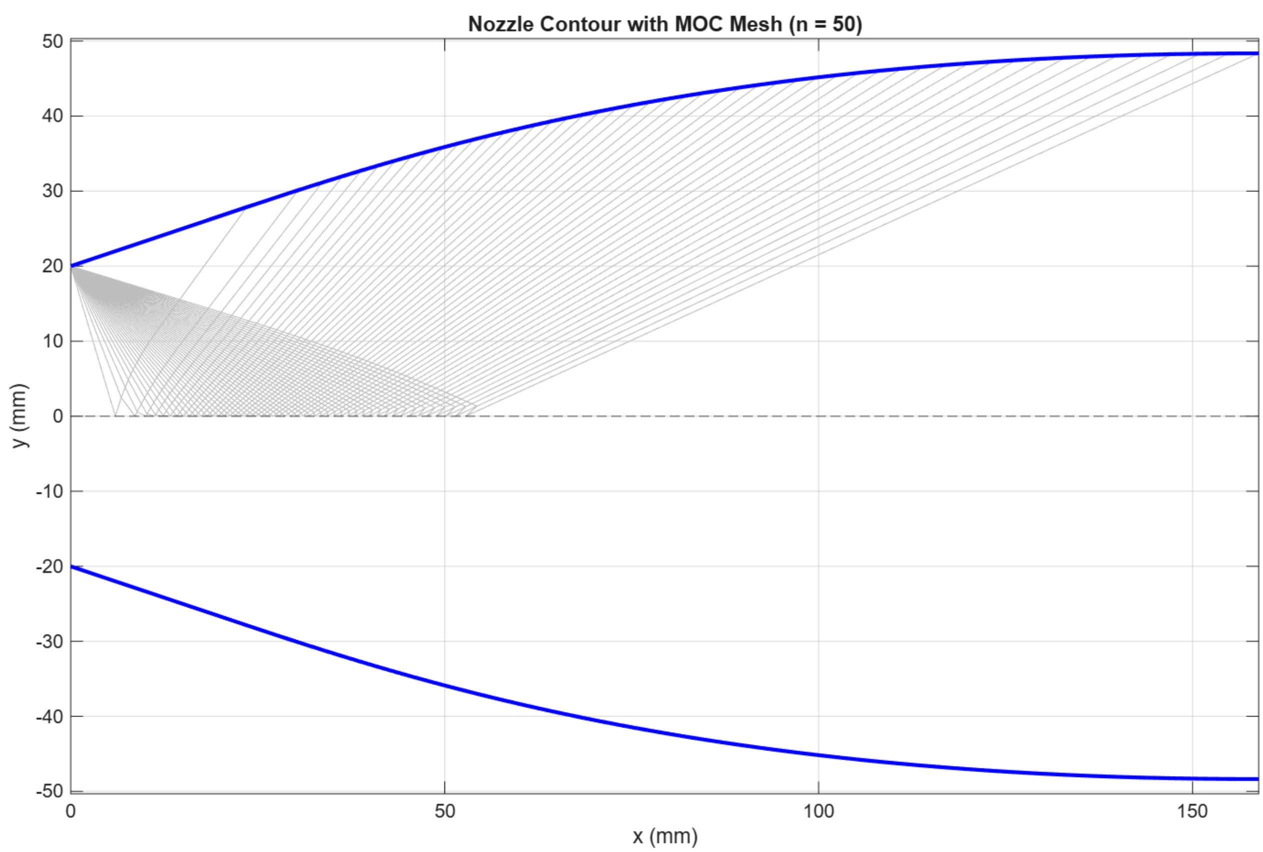

Figure 1: Nozzle Contour with MOC Mesh (n=50)

5.2 Nozzle Contour Coordinates Table

Table 3: Nozzle Contour Coordinates

Pt.	x (m)	y (m)	Pt.	x (m)	y (m)	Pt.	x (m)	y (m)
0	0	0.02	**17**	0.064363	0.039324	**34**	0.105322	0.045756
1	0.023543	0.027875	**18**	0.066493	0.039778	**35**	0.108148	0.046039
2	0.030407	0.030122	**19**	0.068647	0.040222	**36**	0.111032	0.04631
3	0.033619	0.031139	**20**	0.070827	0.040657	**37**	0.113977	0.046567
4	0.036368	0.03199	**21**	0.073036	0.041083	**38**	0.116985	0.046811
5	0.038862	0.032744	**22**	0.075277	0.0415	**39**	0.120058	0.047039
6	0.041199	0.033435	**23**	0.07755	0.041907	**40**	0.123198	0.047252
7	0.043434	0.034079	**24**	0.079859	0.042306	**41**	0.126407	0.047449
8	0.0456	0.034689	**25**	0.082205	0.042696	**42**	0.129688	0.04763
9	0.047721	0.035271	**26**	0.084591	0.043077	**43**	0.133044	0.047792
10	0.049812	0.035831	**27**	0.087018	0.043448	**44**	0.136476	0.047936
11	0.051886	0.036372	**28**	0.089488	0.043809	**45**	0.139988	0.048061
12	0.053951	0.036896	**29**	0.092003	0.04416	**46**	0.143582	0.048166
13	0.056015	0.037405	**30**	0.094565	0.044502	**47**	0.14726	0.048249
14	0.058084	0.037902	**31**	0.097176	0.044832	**48**	0.151027	0.04831
15	0.060162	0.038387	**32**	0.099838	0.045151	**49**	0.154885	0.048347
16	0.062254	0.038861	**33**	0.102553	0.045459	**50**	0.158848	0.04836

5.3 Area Ratio Along the Wall

Figure 2 plots the local area ratio (A/A_{throat}) against the normalized axial position x/L. The curve rises smoothly and monotonically from 1.0 at the throat to 2.418 at the exit, with no local extrema, inflections, or discontinuities in slope. This is a direct geometric consequence of the smooth wall contour in Figure 1. The area ratio increases steeply over the first half of the nozzle, where the flow does most of its turning, then flattens as $x/L \to 1$, approaching uniform, parallel conditions.

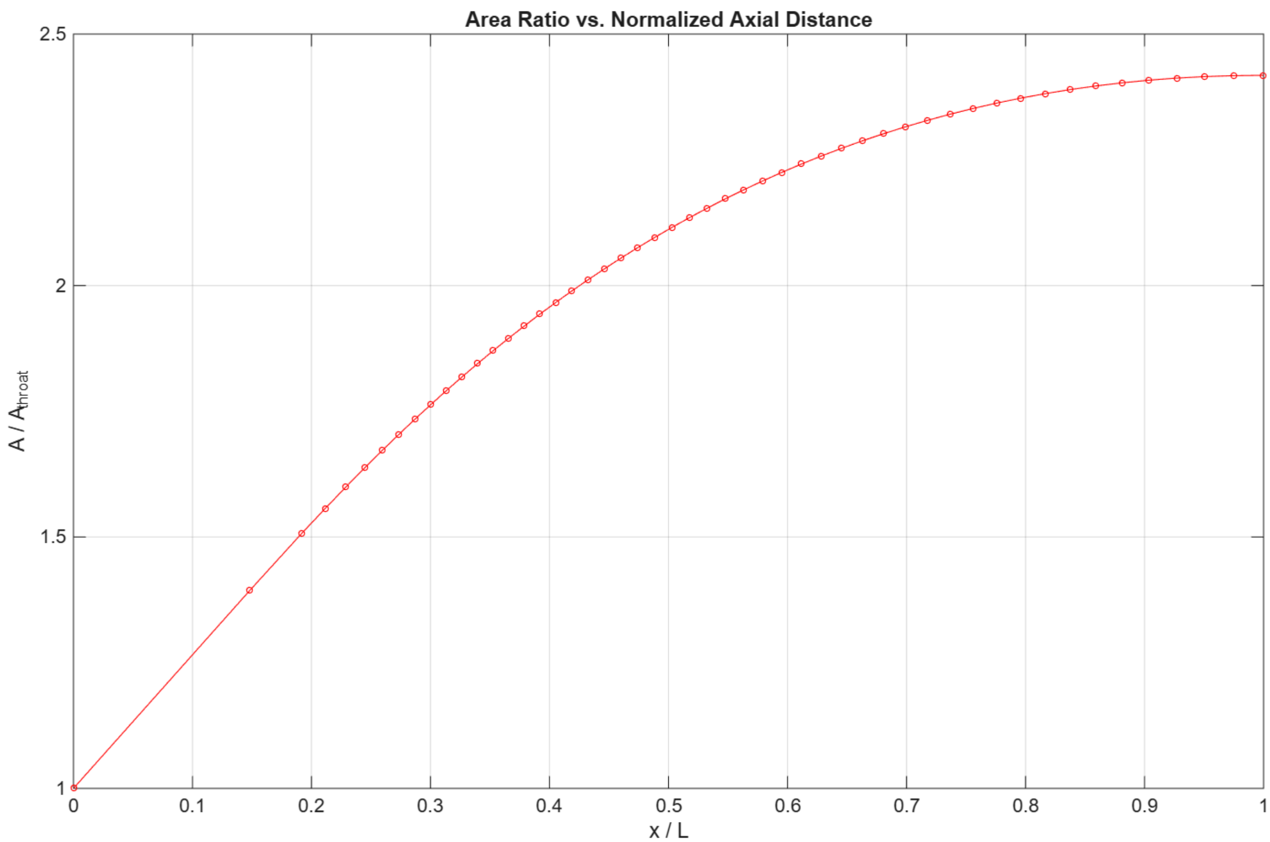

Figure 2: Nozzle Area Ratio Along the Wall

5.4 Flow Properties Along Nozzle Centerline

Figure 3 shows the Mach number, static pressure, and static temperature along the nozzle axis. All three vary smoothly and monotonically from the throat ($M = 1$, $P = 792.4\ kPa$, $T = 833.3\ K$) to their design exit values ($M = 2.410$, $p = 101.0\ kPa$, $T = 462.6\ K$). Notably, the centerline reaches the full design Mach number at $x \approx 52.8\ mm$, roughly a third of the way down the 158.8 mm nozzle, well before the physical exit plane. This is expected because once the flow along the axis has passed the last reflected characteristic, it is already at the design condition, and the remaining nozzle length exists only to bring the flow near the wall up to that same uniform state by the exit.

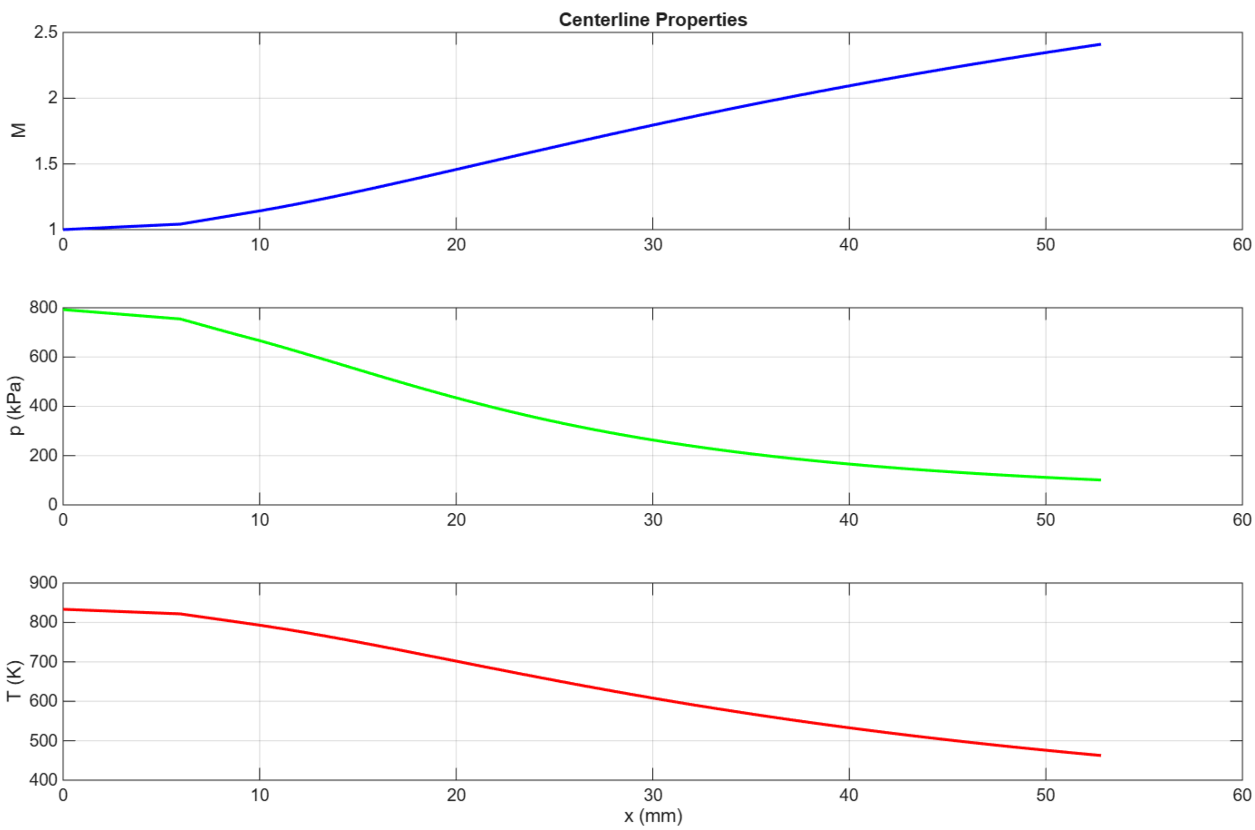

Figure 3: Centerline Properties

5.5 Flow Properties Along Nozzle Wall

Figure 4 shows the same three quantities evaluated along the nozzle wall. Unlike the centerline, the wall properties change most rapidly over the very first segment (the sharp-corner expansion), then vary smoothly and gradually for the remainder of the nozzle. At the exit, the wall values converge to the same state as the centerline ($M = 2.410$, $p = 101.0\ kPa, T = 462.6\ K$), confirming that the flow is uniform and axis-parallel across the entire exit plane, as required by the design specification.

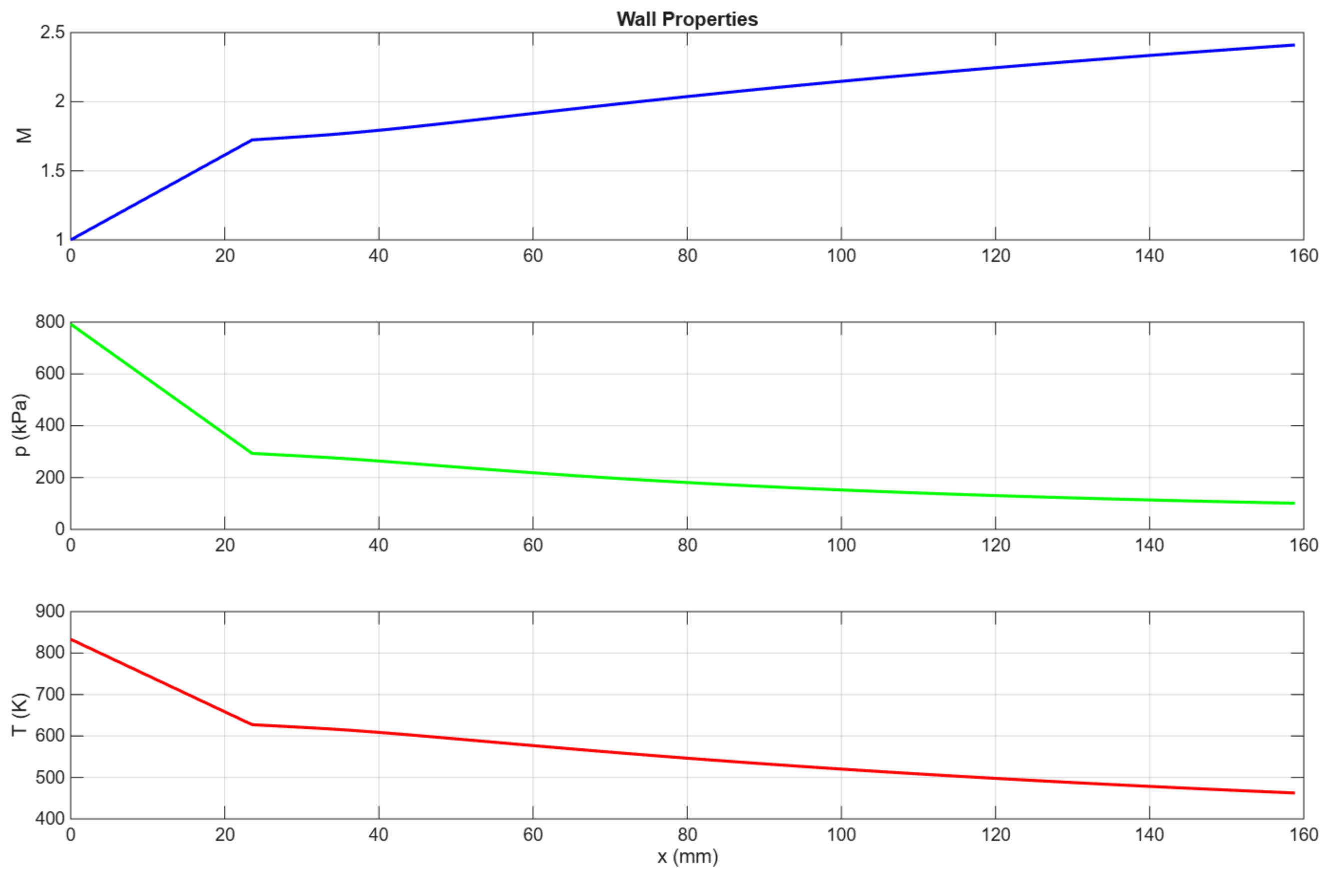

Figure 4: Wall Properties

6. Discussion

The final design fulfills every requirement stated from the very beginning of this project. The nozzle has been designed for optimal expansion, and the static pressure at the exit is set to the ambient value of 101 kPa. The calculated contour has its static pressure values at the exit being equal to this value on both the centerline and the wall (see Figures 3-4). Air has been considered calorically perfect throughout the problem: γ is 1.4, and R is 287 J/kg·K, which has been taken into account in every relation used.

As the minimum-length algorithm destroys all expansion waves that reach the wall, the lack of any waves implies that there are no more factors affecting the flow when the last characteristic moves away. This can be easily checked numerically because on the exit section, the center line and wall will be in the same state (M_e = 2.4101, P_a = 101.0 kPa, T_e = 462.6 K, θ = 0°). Thus, the calculated area ratio A_e/A_t = 2.418, which differs from the 1-D isentropic ratio of 2.4254 just by 0.305% (because of a finite number of grid points, in this case, 50 waves), corresponds to the perfectly expanded gas flow with the highest kinetic energy for the specified ratio of stagnation and ambient pressures. The energy released by the expansion process reaches 53.74% of the stagnation enthalpy. This fraction is the highest possible one, as was stated in Part (b).

After the throat corner, the wall is tapered at decreasing angles of dθ = 0.3699° per 50 steps until 0° is reached (θ_{max} = 18.495°), such that none of these angles can be called large, and the resulting profile will have a continuous monotonic curvature everywhere except at the throat corner. This corner is the sole inescapable exception, the point at which the entire expansion fan is concentrated to achieve the minimum-length geometry. All other changes in geometry are intentionally gradual. The concentration of the expansion here, rather than its spreading out along the longer curve, is also the reason why this is the minimum-length nozzle able to generate shock-free and uniform flow at M_e = 2.4101 (L = 0.158848 m, or $L/r_t \approx 7.94$).

The throat radius, $r_t = 0.02\ m$, was chosen as the input parameter for all geometry and area-ratio calculations throughout this report. This is just an arbitrary value in the sense that it doesn't affect any of the physics involved: M_e, V_e, T_e, the kinetic energy fraction, and A_e/A_t are calculated solely based on the 1-D isentropic relations and Prandtl-Meyer turning angles and are independent of r_t. In other words, changing the value of r_t would only result in rescaling the geometry (x, y, and L) linearly without changing any of the Mach number, pressure, and temperature profiles plotted in Figures 3 and 4. Finally, the slight difference between the calculated and isentropic area-ratio values is attributable to the expected finite-characteristic-mesh behavior. As the number of waves increases when discretizing the expansion fan, the piecewise linear representation of each characteristic wave becomes a better approximation of the actual curvilinear wave. Therefore, this difference is the result of using the finite mesh only. All things considered, the design meets all the specified requirements. Perfect expansion, constant parallel-flow exit, a streamlined shape with no shocks, and the shortest possible length.

7. References

[1] J. D. Anderson, Modern Compressible Flow: With Historical Perspective, 4th ed. New York, NY, USA: McGraw-Hill, 2020.

[2] I. M. Hall, "Inversion of the Prandtl-Meyer relation," Dept. Mechanics of Fluids, Univ. of Manchester, Manchester, U.K., 1975.
http://servidor.demec.ufpr.br/CFD/bibliografia/propulsao/Hall_1975.pdf

[3] K. Lee, "Week 5-4 slideshow," AEE-3162 Compressible Flow, Florida Institute of Technology, Melbourne, FL, USA, Jun. 18, 2026.

[4] E. Andrews, "Aerothermodynamics coursework: Method of characteristics".
https://old.xorgon.me/science/files/MoC.pdf

[5] "Method of characteristics - Lesson 6," Internal Compressible Flows, ANSYS Innovation Space.
https://innovationspace.ansys.com/courses/courses/internal-compressible-flows/lessons/method-of-characteristics-lesson-6/

[6] R. S. Tarnacha and M. Virmani, "Design of rocket engine nozzle using method of characteristics," Int. J. Res. Appl. Sci. Eng. Technol., vol. 12, no. 5, May 2024, doi: 10.22214/ijraset.2024.62512.

[7] M. B. Bush, "Isentropic flow tables, γ = 1.4," 1999.
https://web.iitd.ac.in/~pmvs/courses/mcl341/isentropic_flow.pdf